Classical-physics applications for Finsler b space

Joshua Foster [a], Ralf Lehnert [b],*

[a] Physics Department, Indiana University, Bloomington, IN 47405, USA
[b] Indiana University Center for Spacetime Symmetries, Bloomington, IN 47405, USA

A B S T R A C T

The classical propagation of certain Lorentz-violating fermions is known to be governed by geodesics of a four-dimensional pseudo-Finsler b space parametrized by a prescribed background covector field. This work identifies systems in classical physics that are governed by the three-dimensional version of Finsler b space and constructs a geodesic for a sample non-constant choice for the background covector. The existence of these classical analogues demonstrates that Finsler b spaces possess applications in conventional physics, which may yield insight into the propagation of SME fermions on curved manifolds.

© 2015 The Authors. Published by Elsevier B.V. This is an open access article under the CC BY license (http://creativecommons.org/licenses/by/4.0/). Funded by SCOAP³.

1. Introduction

In Einstein's general relativity, the mathematical description of the classical gravitational field is intrinsically geometric and rests on the concept of a Riemannian manifold. However, in the quest for a consistent quantum theory of gravitation, this phenomenologically successful and elegant geometric formalism may need to be generalized. A popular broader geometric framework that incorporates Riemannian manifolds as a special limit is provided by Riemann–Finsler geometry [1–4]. The recent interest of the physics community in studying such geometries [5–23] has primarily arisen in the context of Lorentz-symmetry violation — a promising phenomenological signature in various theoretical approaches to quantum gravity [24–31].

The Standard-Model Extension (SME) has been developed to describe Lorentz-violating effects at presently attainable energies regardless of their high-energy origin [32,33]. This framework has provided the basis for numerous experimental [34–39] and theoretical [40–43] studies of Lorentz breaking. In particular, one SME study has uncovered the incompatibility of Riemannian (and Riemann–Cartan) geometry with explicit Lorentz violation [33], suggesting Riemann–Finsler spaces as the appropriate geometrical description of Lorentz-violating physics in such situations. Further theoretical evidence supporting this suggestion originates from the classical-particle limit of the SME [44]: the motion of such particles is effectively governed by geodesics in a Riemann–Finsler space [10] despite the presumed underlying Riemannian structure. This analysis also allows a partial classification of the emerging

physically relevant Finsler structures [10] according to the type of Lorentz breakdown. For example, the SME's a^μ coefficient for fermions leads to the familiar Randers space [45].

The present study is primarily concerned with Finsler b space [10], which also emerges from the classical-particle limit of the SME. To define b space and other Finsler structures in a simplified form suitable for our present purposes, we note the following. The aforementioned SME-inspired partial classification of Finsler spaces is based on physical spacetime manifolds. These possess indefinite metrics and are therefore pseudo-Riemannian. For perturbative Lorentz violation, the indefinite-metric feature carries over to the Finsler-geometry interpretation, yielding pseudo-Finsler spaces. In this work, we are primarily concerned with the corresponding Finsler versions of these structures with a positive-definite metric. In particular, the relevant base manifold for our present study is $\mathbb{R}^3$ endowed with the usual Euclidean metric. It then becomes unnecessary to distinguish between vectors and covectors. Moreover, points on the manifold may be interpreted as vectors. In general, we denote vectors as boldface letters.

With these consideration in mind, we recall the common notation for Finsler spaces involving a scalar function F on the tangent bundle: integration of F along a path on the manifold yields the Finsler path length with geodesics defined as extremal paths between fixed points. For example, the Randers-space F function is denoted by F_a and given by

$$F_a(\mathbf{x}, \mathbf{x}') = \rho(\mathbf{x}, \mathbf{x}') + \alpha(\mathbf{x}, \mathbf{x}'), \tag{1}$$

where

$$\rho(\mathbf{x}, \mathbf{x}') = \sqrt{\mathbf{x}'^2},$$
$$\alpha(\mathbf{x}, \mathbf{x}') = \mathbf{a}(\mathbf{x}) \cdot \mathbf{x}'. \tag{2}$$

* Corresponding author.
    E-mail address: ralehner@indiana.edu (R. Lehnert).

Here, $\mathbf{x} = \mathbf{x}(\lambda)$ is a sufficiently well-behaved curve on the manifold, $\mathbf{x}' = \mathbf{x}'(\lambda)$ is the corresponding velocity in the tangent space $T_{\mathbf{x}}M$, and $\mathbf{a}(\mathbf{x})$ is a prescribed (co)vector field. The Finsler structure for b space, on the other hand, is [10]

$$F_b(\mathbf{x}, \mathbf{x}') = \rho(\mathbf{x}, \mathbf{x}') \pm \beta(\mathbf{x}, \mathbf{x}'), \tag{3}$$

where

$$\beta(\mathbf{x}, \mathbf{x}') = \sqrt{\mathbf{b}(\mathbf{x})^2 \mathbf{x}'^2 - \left[\mathbf{b}(\mathbf{x}) \cdot \mathbf{x}'\right]^2}, \tag{4}$$

and $\mathbf{b}(\mathbf{x})$ is a given (co)vector field. It has been argued that b space is in some sense complementary to Randers space [10]. In any case, this Finsler b structure emerges from the classical-particle limit of the SME's b^μ coefficient for fermions. For completeness, we also recall the definition of the Finsler ab structure [10]

$$F_{ab}(\mathbf{x}, \mathbf{x}') = \rho(\mathbf{x}, \mathbf{x}') + \alpha(\mathbf{x}, \mathbf{x}') \pm \beta(\mathbf{x}, \mathbf{x}'), \tag{5}$$

which may be thought of as a combination of Randers and b space.

In the present work, our primary focus is to find systems in classical physics that are governed by the Finsler b structure presented in Eq. (3). The identification of simple table-top systems described by the same set of equations as some less transparent system has long been employed in physics research. Such analogues can give complementary perspectives on and further insight into the original system; they may allow the application of ideas and methods from other fields of physics; they may create opportunities for controlled experimentation within the analogue that can be translated back to the original system; and they can illustrate key physics ideas for educational purposes. Examples of these types of analogues across various sub-disciplines of physics include a number of Randers-space applications, such as Zermelo navigation, optical metrics, and magnetic flow [46]; modeling discrete spacetime-symmetry violations in meson oscillations with mechanical and electric-circuit systems [47]; analogue gravity [48]; models for PT-symmetric quantum mechanics [49]; etc.

This Letter is structured as follows. Section 2 reviews some basics about Finsler b space and sets up our analysis. In Section 3, we present a b-space application involving a bead sliding on a wire. A second system governed by the Finsler b structure, which is based on a transversely polarized magnetic chain, is analyzed in Section 4. Section 5 comments on some aspects of the corresponding geodesics. A brief summary is contained in Section 6.

2. Preliminary considerations

An important consideration in the construction of our classical-physics Finsler examples concerns the dimensionality of the manifold involved. For example, the aforementioned Zermelo navigation problem can be formulated in two dimensions, one of the key features that makes this Randers-space example particularly simple and intuitive. In the present context, it would then seem natural to search also for simple, two-dimensional b-space examples. However, the Finsler structures (1) and (3) are equivalent in two space dimensions [10]. Since our goal is to identify classical-physics analogues governed by true Finsler b spaces, nontrivial examples must involve at least three-dimensional manifolds. Indeed, it can be shown [10] that in three or more dimensions the b-space Matsumoto torsion is non-vanishing. Inequivalence to Randers space then follows directly from the Matsumoto–Hōjō theorem [50].

Another consideration concerns the smoothness of F_b because basic objects, such as the expression for the Finsler metric $g_{jk} = \frac{1}{2} \partial_{x'^j} \partial_{x'^k} F_b^2$, involve derivatives of F_b. Inspection of F_b reveals that it is differentiable everywhere with the exception of an extended slit S given by $x'^j = \kappa b^j$, where $\kappa \in \mathbb{R}$. It has been conjectured

that the geometry at this extended slit can be resolved using standard techniques for singularities of algebraic varieties [10], and progress towards such results has been made [51]. From the perspective of the underlying SME quantum physics, this singularity can likely be addressed by introducing a spin variable [10]. In the present context of classical-physics analogues, we focus on those solutions that do not involve the slit.

For F_b to be a true Finsler structure, some additional conditions need to hold. These include homogeneity of degree one in $\mathbf{x}'$ and positive definiteness of both F_b and the associated Finsler metric g_{jk}. Homogeneity is established by inspection, and positive definiteness requires

$$|\mathbf{b}| < 1 \tag{6}$$

for the lower sign in Eq. (3). We note that this latter constraint is compatible with the underlying motivation of the present analysis: $\mathbf{b}$ represents the analogue of the Lorentz-symmetry violating b^μ coefficient, which must be perturbatively small on experimental grounds.

The construction of classical-physics analogues for Finsler geometry amounts to finding systems governed by a variational principle, i.e., by the extremization of some integral. At first sight, the Principle of Least Action applied to nonrelativistic mechanical systems would appear to be a natural starting point for the identification of such Finsler analogues. However, the presence of the mandatory kinetic-energy term in the Lagrangian L seems to place tight restrictions on the overlap between L and the set of possible Finsler structures F, and we have found that Lagrangians without a kinetic term will typically seem contrived.

Another widely known physics application of the variational method is Fermat's Principle in ray optics. It states that light rays between two fixed points A and B traverse the path of stationary optical length with respect to variations of the path, i.e.,

$$\delta \int_A^B n(\mathbf{x}, \mathbf{x}') \, ds = 0. \tag{7}$$

Here, s denotes the arc length of the light path $\mathbf{x}(s)$, and $n(\mathbf{x}, \mathbf{x}')$ is the refractive index, which may depend on both the position $\mathbf{x}(s)$ and the propagation direction $\mathbf{x}'(s)$ of the light. The prime expresses differentiation with respect to the argument. The spatial dependence of the refractive index $n(\mathbf{x}, \mathbf{x}')$ can now be selected to recover most Finsler structures. Consider, for instance, the choice

$$n(\mathbf{x}, \mathbf{x}') = 1 + \sqrt{\mathbf{b}^2 - (\mathbf{b} \cdot \mathbf{e}_{x'})^2}, \tag{8}$$

where $\mathbf{b}$ is a prescribed vector field, and $\mathbf{e}_{x'}$ denotes the unit vector in the instantaneous propagation direction. With this refractive index and a change of variables to a general, well-behaved path parametrization $s = s(\lambda)$, Eq. (7) takes the form of a classical system governed by Finsler b space. Although direction-dependent refractive indices are not uncommon in physics, it would seem difficult to control experimentally the vector field $\mathbf{b}$: if only a constant $\mathbf{b}$ can be achieved, translational invariance would yield the perhaps less interesting case of straight-line light propagation (see Section 5). In what follows, we seek examples in which $\mathbf{b}$ is freely adjustable, at least in principle.

3. Bead on a wire

As the first classical-physics analogue governed by a Finsler b-space geometry, we consider a bead of mass m that slides in three space dimensions on a rough wire. The bead's position vector as a function of time t is denoted by $\mathbf{x}(t)$. The bead fits tightly
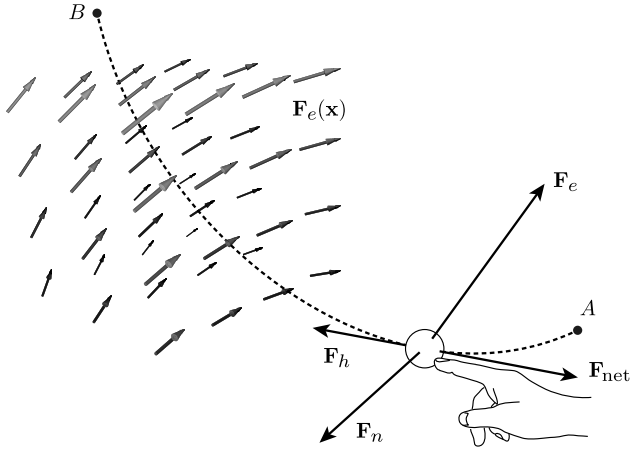
Fig. 1. Bead on a wire. The dashed line represents the wire with endpoints A and B. The figure also shows the external force field $\mathbf{F}_e(\mathbf{x})$ and the free-body diagram for the bead. In the free-body diagram, the dependence of the forces on the position $\mathbf{x}$ is suppressed for brevity.

around the wire, resulting in a frictional force $\mathbf{F}_0$ that is constant in magnitude and directed against the bead's velocity $\mathbf{v}(t) = \dot{\mathbf{x}}(t)$. The dot denotes the derivative with respect to time.

The bead also experiences a prescribed external force $\mathbf{F}_e(\mathbf{x})$. The physical origin of $\mathbf{F}_e(\mathbf{x})$ could, for example, be due to a gravitational field, an electric field (if the bead is charged), forces resulting from the flow of wind or water, etc. This external force and the bead's motion generally require a normal force $\mathbf{F}_n(\mathbf{x})$ perpendicular to $\dot{\mathbf{x}}(t)$ to keep the bead on the wire. This will lead to a further frictional force of magnitude $\mu|\mathbf{F}_n(\mathbf{x})|$ opposing the bead's motion, where μ is a constant coefficient of kinetic friction. This additional friction is assumed to be independent of $\mathbf{F}_0$.

The forces $\mathbf{F}_0$ and $\mathbf{F}_n(\mathbf{x})$, the friction coefficient μ, and the initial conditions may not permit the bead to slide at all. To circumvent this issue, we allow for an additional force $\mathbf{F}_h$ that can only act along the wire. Note in particular that this force can therefore not contribute to the friction. We take $\mathbf{F}_h$ to be adjustable so that certain limiting cases, such as quasistatic motion, can be achieved. In a physical context, $\mathbf{F}_h$ could for example provide the description of a hand moving the bead along the wire.

Given this classical-mechanics system, we now consider the following situation. Given two distinct points A and B in space that represent the two ends of the wire, the bead slides from A to B. Holding A and B fixed, how must the wire be bent for the energy loss ΔE due to friction to be minimal? If the wire is not required to have a given constant length, ΔE can be expressed as

$$\Delta E = -\int_A^B \mathbf{F}_{\text{net}}(\mathbf{x}) \cdot d\mathbf{x}, \tag{9}$$

where $\mathbf{F}_{\text{net}}(\mathbf{x})$ denotes the net friction, and the integration is understood to be carried out along a path $\mathbf{x}(t)$ with end points A and B. The overall minus sign expresses our convention that the energy loss ΔE be positive. Since the friction loss ΔE is associated with abrasive wear, the problem of minimizing ΔE may, for instance, be motivated from an engineering standpoint that seeks to make a mechanical system last longer by reducing abrasive wear. Our set-up is depicted schematically in Fig. 1.

To find an explicit expression for $\mathbf{F}_{\text{net}}(\mathbf{x})$ in terms of the given force field $\mathbf{F}_e(\mathbf{x})$, it is useful to consider Newton's 2nd Law expressed in the Frenet–Serret frame that is comoving with the bead. This frame is as usual composed of the unit vector $\mathbf{T}(t)$ tangent to the path $\mathbf{x}(t)$, the unit normal vector $\mathbf{N}(t)$ pointing in the di-

rection of $\dot{\mathbf{T}}(t)$ perpendicular to $\mathbf{T}(t)$, and the binormal vector $\mathbf{B}(t) \equiv \mathbf{T}(t) \times \mathbf{N}(t)$. In the TNB basis, the bead's acceleration is given by $\ddot{\mathbf{x}}(t) = \dot{v}(t)\mathbf{T}(t) + v(t)|\dot{\mathbf{T}}(t)|\mathbf{N}(t)$. Suppressing the time and space dependence for brevity and denoting vector components in the $\mathbf{T}$, $\mathbf{N}$, and $\mathbf{B}$ directions with the respective superscripts T, N, and B, Newton's 2nd Law takes the following form:

$$F_e^T + F_h^T - |\mathbf{F}_0| - \mu|\mathbf{F}_n| = m\dot{v} \tag{10}$$

$$F_e^N + F_n^N = mv|\dot{\mathbf{T}}| \tag{11}$$

$$F_e^B + F_n^B = 0. \tag{12}$$

Equations (11) and (12) can be solved for the normal-force components F_n^N and F_n^B. With these components at hand, the net frictional force becomes

$$\mathbf{F}_{\text{net}} = -\big(|\mathbf{F}_0| + \mu|\mathbf{F}_n|\big)\mathbf{T}$$
$$= -\left[|\mathbf{F}_0| + \mu\sqrt{\left(F_e^N - mv|\dot{\mathbf{T}}|\right)^2 + \left(F_e^B\right)^2}\right]\mathbf{T}, \tag{13}$$

where we have used that kinetic friction acts in the direction opposite to the velocity.

We are now in a position to express the integral (9) to be minimized in terms of $\mathbf{F}_e$. The following change of variables $d\mathbf{x} = \dot{\mathbf{x}}dt = v\mathbf{T}dt$ gives

$$\Delta E = \int_A^B v\left[|\mathbf{F}_0| + \mu\sqrt{\left(F_e^N - mv|\dot{\mathbf{T}}|\right)^2 + \left(F_e^B\right)^2}\right]dt. \tag{14}$$

We now proceed by considering two limiting cases of this expression, each governed by a Finsler b-space geometry.

The first case is the zero-mass limit, which eliminates the centripetal-force term in Eq. (14). The square-root expression can then readily be identified with the magnitude of the force $\mathbf{F}_e^\perp = \mathbf{F}_e - v^{-2}(\mathbf{F}_e \cdot \dot{\mathbf{x}})\dot{\mathbf{x}}$, which is the component of $\mathbf{F}_e$ perpendicular to the wire, i.e., $\mathbf{F}_e^\perp \cdot \dot{\mathbf{x}} = 0$. Recalling $v = \sqrt{\dot{\mathbf{x}}^2}$, we find

$$\Delta E = \int_A^B \left[|\mathbf{F}_0|\sqrt{\dot{\mathbf{x}}^2} + \mu\sqrt{\mathbf{F}_e^2\dot{\mathbf{x}}^2 - (\mathbf{F}_e \cdot \dot{\mathbf{x}})^2}\right]dt \tag{15}$$

for the energy loss due to friction. It is apparent that with the identification $\mathbf{b} = \mu|\mathbf{F}_0|^{-1}\mathbf{F}_e$, we recover F_b defined in Eq. (3) up to an overall factor. Thus, the zero-mass limit of our bead sliding on a wire indeed provides a classical-physics situation described by the Finsler b structure when the energy loss is to be minimized.

Alternatively, we may consider the limit of quasistatic motion, in which the bead is understood to move with a speed $v \to 0$. This situation can, for example, be created if the bead is moved slowly by hand along the wire, which can be modeled by adjusting $\mathbf{F}_h$ such that the left-hand side of Eq. (10), and thus $\dot{v}$, vanish. A slow initial speed then remains unchanged. The direct implementation of the $v \to 0$ limit in Eq. (14) lacks clarity because the integrand exhibits a multiplicative factor of v. We therefore change integration variables from time t to arc length s, so that the offending v factor is absorbed into the integration measure $v\,dt = ds$. The limit is now more transparent; it again eliminates the centripetal-force contribution:

$$\Delta E = \int_A^B \left[|\mathbf{F}_0| + \mu\sqrt{\mathbf{F}_e^2 - (\mathbf{F}_e \cdot \mathbf{x}')^2}\right]ds, \tag{16}$$

where the prime denotes differentiation with respect to s. With the same identification $\mathbf{b} = \mu|\mathbf{F}_0|^{-1}\mathbf{F}_e$ as before, we recover up
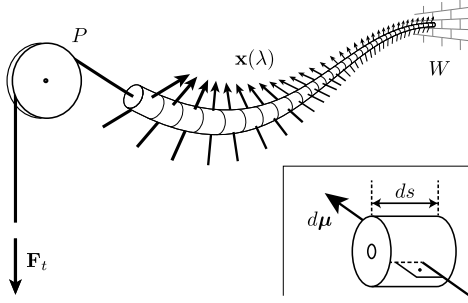
Fig. 2. Magnetic beads on a string. At the point W, the string is attached to a wall. Its other end hangs over a pulley at point P and is held under a constant tension $\mathbf{F}_t$. The beads are threaded tightly on the string. They are free to rotate about the string with their magnetic moments remaining perpendicular to the string. The external $\mathbf{B}$ field is not shown. The inset depicts the close-up of a single bead.

to an overall factor the arc-length version of F_b given in Eq. (3). We therefore conclude that the quasistatic limit of our bead-on-a-wire example also provides a classical-physics analogue for Finsler b space.

4. Transversely magnetized chain

To establish a second classical-physics situation described by a Finsler b-space structure, we consider a catenary-type problem in three space dimensions. More specifically, we examine the shape of a chain under the influence of magnetic forces in static equilibrium.

The chain consists of beads that are threaded on a string. This threading is tight in the sense that neighboring beads are in contact with one another. This is to prevent motion of the beads along the string. However, the beads are allowed to rotate freely and independently about the string. The beads are identical. They carry a magnetic dipole moment $d\boldsymbol{\mu}$ that is oriented perpendicular to their symmetry axis and thus remains perpendicular to the string (see Fig. 2). At the point W, this magnetic chain is held fixed, for example, by attaching it to a wall. The other end of the chain hangs over a pulley P and is kept under constant tension $\mathbf{F}_t$. Such a force might be provided by tensioning with a weight. This set-up is depicted in Fig. 2. The segment of the chain between P and W is exposed to a time-independent external magnetic field $\mathbf{B}(\mathbf{x})$. The question to be addressed concerns the equilibrium shape $\mathbf{x}(\lambda)$ of this magnetic chain.

To find an equation for the equilibrium shape, we note that a static, stable configuration minimizes the total potential energy E of the system. Our magnetic-chain set-up allows for various contributions to E. To make the problem tractable, we idealize the set-up by neglecting the following contributions. First, we consider the string and the beads to be inelastic so as to preclude energy storage in the chain by stretching or compressing. As the second idealization, we take the string and the beads to be massless so that gravity can be ignored. The third effect we neglect concerns the dipole–dipole interactions between different beads.[1]

In what follows, we focus on two contributions to the potential energy E. One of these arises as a result of the tension $\mathbf{F}_t$ applied to the string. This tension implies that any deformation of the chain away from the straight-line configuration between W and P requires work to be done against $\mathbf{F}_t$, which is then stored as potential energy E_t in the system. Since $\mathbf{F}_t$ is constant, E_t increases linearly with the length of chain drawn across the pulley. Selecting a convenient energy zero, we thus find

$$E_t = F_t \int\limits_W^P \sqrt{\mathbf{x}'(\lambda) \cdot \mathbf{x}'(\lambda)}\, d\lambda\,, \tag{17}$$

where F_t denotes the magnitude of $\mathbf{F}_t$, and λ is a general parameter along the chain such that $\mathbf{x}(\lambda)$ is sufficiently well-behaved.

The second contribution is a result of the magnetic interaction between the externally prescribed $\mathbf{B}(\mathbf{x})$ and the individual magnetic moments $d\boldsymbol{\mu}(\mathbf{x})$ of the beads. A single bead at $\mathbf{x}$ possesses an energy $dE_B(\mathbf{x})$ given by [52]:

$$dE_B(\mathbf{x}) = -\mathbf{B}(\mathbf{x}) \cdot d\boldsymbol{\mu}(\mathbf{x})\,. \tag{18}$$

This expression shows that the net magnetic energy of the chain will consist of two contributions: the orientation of the beads' magnetic momenta and the shape of the chain.

As a first step, we consider an arbitrary fixed shape $\mathbf{x}(\lambda)$ of the chain. The interaction (18) causes a torque on the dipole in such a way as to align it with the magnetic field.[2] But as the beads are only allowed to rotate about one axis (i.e., the fixed string), the alignment is not necessarily perfect. Rather, the beads rotate such that the angle $\theta(\mathbf{x})$ between each bead's magnetic moment and the external magnetic field $\mathbf{B}(\mathbf{x})$ at the bead's position is minimized. In particular, $0 \le \theta(\mathbf{x}) \le 90°$ and $d\boldsymbol{\mu}(\mathbf{x})$ lies in the plane spanned by $\mathbf{B}(\mathbf{x})$ and the tangent $d\mathbf{x}$ to the curve $\mathbf{x}(\lambda)$.[3] In this stable configuration, we therefore have

$$\cos\theta(\mathbf{x}) = \sin\phi(\mathbf{x}) = +\sqrt{1 - \cos^2\phi(\mathbf{x})}\,, \tag{19}$$

where $\phi(\mathbf{x})$ is the angle between $\mathbf{B}(\mathbf{x})$ and $d\mathbf{x}$. Since the beads on our magnetic chain are identical, we can take the linear magnetic-moment density $\zeta = d\mu/ds$ to be constant and write $d\boldsymbol{\mu}(\mathbf{x}) = \zeta\, ds$ for the magnitude $d\mu$ of the magnetic moment. With these considerations, Eq. (18) becomes

$$dE_B(\mathbf{x}) = -B(\mathbf{x})\, \zeta\, ds\, \sqrt{1 - \cos^2\phi(\mathbf{x})}$$
$$= -\zeta \sqrt{\mathbf{B}(\mathbf{x})^2\, d\mathbf{x}^2 - \big[\mathbf{B}(\mathbf{x}) \cdot d\mathbf{x}\big]^2}\,. \tag{20}$$

For a given shape $\mathbf{x}(\lambda)$, this yields

$$E_B = -\zeta \int\limits_W^P \sqrt{\mathbf{B}(\mathbf{x})^2\, \mathbf{x}'(\lambda)^2 - \big[\mathbf{B}(\mathbf{x}) \cdot \mathbf{x}'(\lambda)\big]^2}\, d\lambda \tag{21}$$

for the chain's net magnetic energy when the dipole beads are aligned in their stable orientation.

With the results (17) and (21) at hand, the total energy E of the chain is given by

$$E = F_t \int\limits_W^P \left[\sqrt{\mathbf{x}'^2} - \frac{\zeta}{F_t} \sqrt{\mathbf{B}^2 \mathbf{x}'^2 - (\mathbf{B} \cdot \mathbf{x}')^2} \right] d\lambda\,, \tag{22}$$

---

[1] The physical consistency of neglecting the dipole–dipole interactions may not be obvious. Consider a set-up of discrete dipoles with finite $\Delta\mu$ separated by a finite Δs. This set-up closely resembles the actual physical situation at microscopic scales involving atoms. Then, a single dipole in an external $\mathbf{B}$ field possesses energy $\Delta E_B \sim B \Delta\mu$, whereas its interaction with one of its neighboring dipoles contributes $\Delta E_{d-d} \sim \Delta\mu^2 \Delta s^{-3}$. The $\mathbf{B}$ field can then always be selected such that ΔE_{d-d} is negligible and can be dropped, at least in principle. To obtain a mathematically more tractable continuum description, we can now approximate the fundamentally discrete sum over ΔE_B by a suitable integral. Note, however, that ignoring the atomistic nature of matter by taking $\Delta s \to 0$ would lead to a diverging ΔE_{d-d} for a constant linear dipole density $\Delta\mu/\Delta s$.

[2] There can also be a net force on the dipole if $\mathbf{B}$ is inhomogeneous.

[3] On the slit described in Section 2, which corresponds to situations in which $\mathbf{B}(\mathbf{x})$ is tangential to $\mathbf{x}(\lambda)$, this is ill-defined. As per our earlier discussion, we exclude such cases from our analysis.

where the dependence of $\mathbf{x}'$ and $\mathbf{B}$ on the curve $\mathbf{x}(\lambda)$ is understood. The equilibrium shape of our magnetic chain is now obtained by minimizing E. Note that with the identification $\mathbf{b} = \zeta \mathbf{B}/F_t$, this system is governed by a Finsler b-space geometry. We remark in passing that Eq. (22) is subject to the physical requirement of $\nabla \cdot \mathbf{B} = 0$ arising from the Maxwell equations.

The above catenary-type system can readily be modified or extended to represent other Finsler structures. For example, a longitudinally magnetized chain would yield a Randers system. A more elaborate bead structure involving transverse magnetic moments, as before, as well as longitudinal electric-dipole moments, would be governed by the F_{ab} Finsler structure (5) with external electric and magnetic fields playing the role of the prescribed $\mathbf{a}$ and $\mathbf{b}$ covector fields, respectively.

5. Sample geodesic solution

Thus far, we have identified two classical-physics systems that are governed by Finsler b space. From a physics perspective, this merely corresponds to setting the problem up. Another interesting question concerns the solution of this problem, i.e., finding the Finsler geodesics for a given $\mathbf{b}(\mathbf{x})$. This section briefly comments on this task.

Under mild assumptions, the b-space extremization problem

$$\delta \int_A^B F_b\big(\mathbf{x}(\lambda), \mathbf{x}'(\lambda)\big) \, d\lambda = 0 \qquad (23)$$

can be converted into a system of three ordinary differential equations. To this end, we employ the usual Euler–Lagrange equations

$$\frac{\partial F_b}{\partial x_j} = \frac{d}{d\lambda} \frac{\partial F_b}{\partial x'_j} \qquad (24)$$

to obtain:

$$\nabla \beta = \pm \left(\frac{\mathbf{x}''}{\rho} - \frac{\mathbf{x}' \cdot \mathbf{x}''}{\rho^3} \mathbf{x}' \right) + \frac{d}{d\lambda} \frac{1}{\beta} \big[b^2 \mathbf{x}' - (\mathbf{b} \cdot \mathbf{x}') \mathbf{b} \big]. \qquad (25)$$

Here, the upper and lower sign choice corresponds to that in Eq. (3). In general, this system of equations is likely to be intractable. However, we may find solutions for special choices for $\mathbf{b}(\mathbf{x})$.

Consider first the case of a constant $\mathbf{b}$. This case can be used to illustrate that our simple analogue models can provide insight into Finsler b space. In our magnetized-chain example, $\mathbf{b} = \text{const.}$ corresponds to a homogeneous magnetic field, which does not exert any forces on the dipoles. We therefore expect that the equilibrium shape of the chain is a straight line.

To see this more rigorously note that the left-hand side of Eq. (24) vanishes, and thus

$$\frac{\partial F_b}{\partial \mathbf{x}'} = \left(\frac{1}{\rho} \pm \frac{b^2}{\beta} \right) \mathbf{x}' \mp \frac{\mathbf{x}' \cdot \mathbf{b}}{\beta} \mathbf{b} = \mathbf{C}, \qquad (26)$$

where $\mathbf{C}$ is a constant. Contraction of this equation with $\mathbf{b}$ yields

$$\mathbf{x}' \cdot \mathbf{b} = \rho \mathbf{C} \cdot \mathbf{b} = \rho c, \qquad (27)$$

with the constant c defined as $c \equiv \mathbf{C} \cdot \mathbf{b}$. Using Eq. (27), all occurrences of the scalar product $\mathbf{x}' \cdot \mathbf{b}$ in Eq. (26) can be traded for ρc. A rearrangement of terms in Eq. (26) then gives

$$\frac{\mathbf{x}'}{\rho} = \left(1 \pm \frac{b^2}{\sqrt{b^2 - c^2}} \right)^{-1} \left(\mathbf{C} \pm \frac{c}{\sqrt{b^2 - c^2}} \mathbf{b} \right). \qquad (28)$$

Since the right-hand side of this equation is constant, we conclude that the unit vector in tangential direction $\mathbf{x}'/\rho$ is constant as well, so $\mathbf{x}(\lambda)$ must be a straight line with respect to our Euclidean base manifold. This result is consistent with the flat-spacetime SME's pseudo-Finsler case, in which free fermions with a constant Lorentz-violating b^μ coefficient also travel along straight paths.

Although straight-line solutions are analogous to fermion propagation in the Minkowski-space SME, it might also be interesting to find sample solutions that do not represent a straight path in the Euclidean base manifold. To this end, consider a $\mathbf{b}(\mathbf{x})$ field with the following cylinder symmetry:

$$\mathbf{b}(\mathbf{x}) = \big[b_0 \exp(-\sigma \varrho) - 1 \big] \hat{\boldsymbol{\varrho}}, \qquad (29)$$

where ϱ denotes the radial cylinder coordinate and $\hat{\boldsymbol{\varrho}}$ is the unit vector associated to ϱ. The range for the parameters b_0 and σ is given by

$$1 < b_0 < 2, \qquad 0 < \sigma. \qquad (30)$$

These constraints guarantee the positivity requirement (6) and the existence of a nonvanishing cylindrical region

$$0 < \varrho < \sigma^{-1} \ln b_0, \qquad (31)$$

in which $\mathbf{b}(\mathbf{x})$ points *away* from the z axis. It is this cylindrical region in which we seek helix solutions of the general form

$$\mathbf{x}(\lambda) = R \cos \lambda \, \hat{\mathbf{x}} + R \sin \lambda \, \hat{\mathbf{y}} + \frac{h}{2\pi} (\lambda - \lambda_0) \, \hat{\mathbf{z}}. \qquad (32)$$

To be located in the region (31), the helix radius $R > 0$ must obey

$$0 < R < \sigma^{-1} \ln b_0 < \sigma^{-1}. \qquad (33)$$

Here, the last of these inequalities follows from the requirement (30). The parameter $h \in \mathbb{R}$ controls the handedness and the pitch of the helix, and $\lambda_0 \in \mathbb{R}$ the offset along the z axis.

With these definitions, the geodesic equation (25) with the upper, positive sign selected is satisfied if

$$|h| = 2\pi R \sqrt{(\sigma R)^{-1} - 1}. \qquad (34)$$

Together with the relation (33), this implies

$$|h| > 2\pi \sigma^{-1} \ln b_0. \qquad (35)$$

In view of the parameter ranges (30), this solution is indeed a proper helix and not a circle $h = 0$. It is also apparent that both handedness choices are acceptable. Note that λ_0 is left unconstrained by the geodesic equation, as expected from translational symmetry of $\mathbf{b}(\mathbf{x})$ along the z axis. We also note that the Finsler b structure is left invariant under $\mathbf{b}(\mathbf{x}) \to -\mathbf{b}(\mathbf{x})$. This observation implies that the established helix solution also solves the upper-sign version of Eq. (25) for an external field $\mathbf{b}(\mathbf{x}) = -\big[b_0 \exp(-\sigma \varrho) - 1 \big] \hat{\boldsymbol{\varrho}}$.

The derivation of the above solution has assumed the case in which β enters the Finsler structure (3) with a plus sign. To find a nontrivial solution for the other sign choice, we consider the same expression (29) for the external field, but we focus on the region in which $\mathbf{b}(\mathbf{x})$ points *towards* the z axis. Positivity (6) holds if

$$0 < b_0 < 2, \qquad 0 < \sigma. \qquad (36)$$

As opposed to the analogous expressions (30), this range has been chosen solely to guarantee the positivity condition (6); no additional restrictions are needed since there is always a nonvanishing region

$$\max(0, \sigma^{-1} \ln b_0) < \varrho \qquad (37)$$

with the desired directionality of $\mathbf{b}(\mathbf{x})$. We again seek helix solutions of the form (32), so we must have

$$\max(0, \sigma^{-1} \ln b_0) < R \tag{38}$$

to be in the region of interest. The geodesic equation, now with the lower, negative sign, yields again Eq. (34). However, since the parameter space for R has changed from the range (33) to the range (38), a real-valued $|h|$ is no longer automatic; we must impose

$$R \leq \sigma^{-1}. \tag{39}$$

Nevertheless, the inequalities (38) and (39) admit a finite range for R. They now also allow the case $h = 0$. As before, λ_0 is left undetermined, and invariance under $\mathbf{b}(\mathbf{x}) \to -\mathbf{b}(\mathbf{x})$ implies that the flipped external field $\mathbf{b}(\mathbf{x}) = -\left[b_0 \exp(-\sigma\varrho) - 1\right]\hat{\boldsymbol{\varrho}}$ leads to the same helix solution.

6. Summary

This work has considered a particular class of Finsler spaces called b space. This Finsler class is complementary to the widely known Randers space and arises in its pseudo-Finsler version as the classical limit of SME fermion propagation. We have shown that three-dimensional b spaces also have other applications in conventional classical physics.

One of these applications involves a bead sliding under friction and external forces on a wire. The shape of the wire that minimizes abrasive forces follows a Finsler b-space geodesic. In this example, the β term enters the expression (3) for F_b with a plus sign. The physical origin of this sign arises from the fact that this β term describes heat generated by friction, which is always dissipative.

The second example we have discussed concerns a transversely magnetized chain in an external magnetic field: the static-equilibrium configuration of the chain is governed by a length-minimizing path with respect to a Finslerian b metric. In this set-up, β enters the expression (3) for F_b with a negative sign for the following physical reason. The β term models the magnetic potential energy of the beads according to Eq. (18). Since the dipoles are free to rotate about the string, the lowest-energy configuration (away from the slit) is always characterized by an acute angle between the dipole and the $\mathbf{B}$ field. This implies a negative magnetic energy for each bead.

The general solution for the geodesic curve for a given $\mathbf{b}(\mathbf{x})$ would be interesting, but appears to be difficult to determine. However, for the sample cases of a constant $\mathbf{b}$ and a $\mathbf{b}(\mathbf{x})$ with a particular cylinder symmetry we have identified nontrivial geodesics.

Acknowledgements

References

[1] B. Riemann, Über die Hypothesen welche der Geometrie zu Grunde liegen, in: R. Baker, C. Christensen, H. Orde (Eds.), Bernhard Riemann, Collected Papers, Kendrick Press, Heber City, UT, 2004.

[2] P. Finsler, Über Kurven und Flächen in allgemeinen Räumen, University of Göttingen dissertation, 1918, Verlag Birkhäuser, Basel, Switzerland, 1951.

[3] D. Bao, S.-S. Chern, Z. Shen, An Introduction to Riemann–Finsler Geometry, Springer, New York, 2000.

[4] S.-S. Chern, Z. Shen, Riemann–Finsler Geometry, World Scientific, Singapore, 2005.

[5] G.Yu. Bogoslovsky, H.F. Goenner, Gen. Relativ. Gravit. 31 (1999) 1383;
G.Yu. Bogoslovsky, H.F. Goenner, Phys. Lett. A 244 (1998) 222;
G.Yu. Bogoslovsky, H.F. Goenner, Gen. Relativ. Gravit. 31 (1999) 1565;
G.Yu. Bogoslovsky, H.F. Goenner, Phys. Lett. A 323 (2004) 40;
G.Yu. Bogoslovsky, Phys. Lett. A 350 (2006) 5;
G.Yu. Bogoslovsky, Int. J. Geom. Methods Mod. Phys. 9 (2012) 1250007;
V. Balan, et al., J. Mod. Phys. 3 (2012) 1314.

[6] F. Girelli, S. Liberati, L. Sindoni, Phys. Rev. D 75 (2007) 064015;
L. Sindoni, Phys. Rev. D 77 (2008) 124009.

[7] G.W. Gibbons, J. Gomis, C.N. Pope, Phys. Rev. D 76 (2007) 081701.

[8] C. Lämmerzahl, D. Lorek, H. Dittus, Gen. Relativ. Gravit. 41 (2009) 1345;
C. Lämmerzahl, V. Perlick, W. Hasse, Phys. Rev. D 86 (2012) 104042.

[9] J. Skákala, M. Visser, Int. J. Mod. Phys. D 19 (2010) 1119;
J. Skákala, M. Visser, J. Geom. Phys. 61 (2011) 1396;
J. Skákala, M. Visser, Class. Quantum Gravity 28 (2011) 065007.

[10] V.A. Kostelecký, Phys. Lett. B 701 (2011) 137.

[11] S.I. Vacaru, Class. Quantum Gravity 28 (2011) 215001.

[12] N. Voicu, Prog. Electromagn. Res. 113 (2011) 83.

[13] J.M. Romero, O. Sanchez-Santos, J.D. Vergara, Phys. Lett. A 375 (2011) 3817.

[14] C. Pfeifer, M.N.R. Wohlfarth, Phys. Rev. D 84 (2011) 044039.

[15] E. Caponio, M.A. Javaloyes, A. Masiello, Math. Ann. 351 (2011) 365;
E. Caponio, M.A. Javaloyes, M. Sánchez, Rev. Mat. Iberoam. 27 (2011) 919;
M.A. Javaloyes, M. Sánchez, Ann. Sc. Norm. Super. Pisa, Cl. Sci. (5) 13 (2014) 813;
A.B. Aazami, M.A. Javaloyes, arXiv:1410.7595;
M.A. Javaloyes, H. Vitório, arXiv:1412.0465.

[16] N.E. Mavromatos, Phys. Rev. D 83 (2011) 025018;
N.E. Mavromatos, S. Sarkar, A. Vergou, Phys. Lett. B 696 (2011) 300;
N.E. Mavromatos, V.A. Mitsou, S. Sarkar, A. Vergou, Eur. Phys. J. C 72 (2012) 1956.

[17] D. Colladay, P. McDonald, Phys. Rev. D 85 (2012) 044042.

[18] Z. Chang, X. Li, S. Wang, arXiv:1201.1368;
Z. Chang, S. Wang, Eur. Phys. J. C 72 (2012) 2165.

[19] P. Stavrinos, Gen. Relativ. Gravit. 44 (2012) 3029;
A.P. Kouretsis, M. Stathakopoulos, P.C. Stavrinos, Phys. Rev. D 86 (2012) 124025.

[20] V.A. Kostelecký, N. Russell, R. Tso, Phys. Lett. B 716 (2012) 470;
N. Russell, arXiv:1501.02490 [hep-th].

[21] R.G. Torromé, arXiv:1207.3791.

[22] J.E.G. Silva, C.A.S. Almeida, Phys. Lett. B 731 (2014) 74.

[23] M. Schreck, arXiv:1405.5518 [hep-th];
M. Schreck, arXiv:1409.1539 [hep-th].

[24] V.A. Kostelecký, S. Samuel, Phys. Rev. D 39 (1989) 683;
V.A. Kostelecký, R. Potting, Nucl. Phys. B 359 (1991) 545;
K. Hashimoto, M. Murata, PTEP, Proces. Teh. Energ. Poljopr. 2013 (2013) 043B01.

[25] I. Mocioiu, M. Pospelov, R. Roiban, Phys. Lett. B 489 (2000) 390;
S.M. Carroll, et al., Phys. Rev. Lett. 87 (2001) 141601;
C.E. Carlson, C.D. Carone, R.F. Lebed, Phys. Lett. B 518 (2001) 201;
A. Anisimov, T. Banks, M. Dine, M. Graesser, Phys. Rev. D 65 (2002) 085032.

[26] V.A. Kostelecky, R. Lehnert, M.J. Perry, Phys. Rev. D 68 (2003) 123511;
R. Jackiw, S.-Y. Pi, Phys. Rev. D 68 (2003) 104012;
O. Bertolami, R. Lehnert, R. Potting, A. Ribeiro, Phys. Rev. D 69 (2004) 083513.

[27] J. Alfaro, H.A. Morales-Técotl, L.F. Urrutia, Phys. Rev. Lett. 84 (2000) 2318;
F.R. Klinkhamer, C. Rupp, Phys. Rev. D 70 (2004) 045020;
G. Amelino-Camelia, et al., AIP Conf. Proc. 758 (2005) 30;
N.E. Mavromatos, Lect. Notes Phys. 669 (2005) 245.

[28] C.D. Froggatt, H.B. Nielsen, arXiv:hep-ph/0211106.

[29] J.D. Bjorken, Phys. Rev. D 67 (2003) 043508.

[30] C.P. Burgess, et al., J. High Energy Phys. 0203 (2002) 043;
A.R. Frey, J. High Energy Phys. 0304 (2003) 012;
J.M. Cline, L. Valcárcel, J. High Energy Phys. 0403 (2004) 032.

[31] V.A. Kostelecký, S. Samuel, Phys. Rev. D 42 (1990) 1289;
N. Arkani-Hamed, et al., J. High Energy Phys. 0405 (2004) 074;
M.V. Libanov, V.A. Rubakov, J. High Energy Phys. 0508 (2005) 001;
G. Dvali, O. Pujolas, M. Redi, Phys. Rev. D 76 (2007) 044028;
S. Dubovsky, P. Tinyakov, M. Zaldarriaga, J. High Energy Phys. 0711 (2007) 083.

[32] D. Colladay, V.A. Kostelecký, Phys. Rev. D 55 (1997) 6760;
D. Colladay, V.A. Kostelecký, Phys. Rev. D 58 (1998) 116002.

[33] V.A. Kostelecký, Phys. Rev. D 69 (2004) 105009.

[34] For an overview of various tests of Lorentz symmetry see V.A. Kostelecký, N. Russell, Rev. Mod. Phys. 83 (2011) 11; 2015 edition: arXiv:0801.0287v8.

[35] See, e.g., S.R. Coleman, S.L. Glashow, Phys. Lett. B 405 (1997) 249;
T. Jacobson, S. Liberati, D. Mattingly, Phys. Rev. D 66 (2002) 081302;
R. Lehnert, Phys. Rev. D 68 (2003) 085003;
F.R. Klinkhamer, M. Schreck, Phys. Rev. D 78 (2008) 085026;
S.T. Scully, F.W. Stecker, Astropart. Phys. 31 (2009) 220.

[36] V.A. Kostelecký, M. Mewes, Phys. Rev. D 66 (2002) 056005;
     R. Lehnert, R. Potting, Phys. Rev. Lett. 93 (2004) 110402;
     R. Lehnert, R. Potting, Phys. Rev. D 70 (2004) 125010;
     V.A. Kostelecký, M. Mewes, Phys. Rev. D 80 (2009) 015020;
     A.A. Abdo, et al., Science 323 (2009) 1688.
[37] V.A. Kostelecký, R. Potting, Phys. Rev. D 51 (1995) 3923;
     M.A. Hohensee, et al., Phys. Rev. Lett. 102 (2009) 170402;
     M.A. Hohensee, et al., Phys. Rev. D 80 (2009) 036010;
     B. Altschul, Phys. Rev. D 80 (2009) 091901;
     G. Amelino-Camelia, et al., Eur. Phys. J. C 68 (2010) 619;
     J.-P. Bocquet, et al., Phys. Rev. Lett. 104 (2010) 241601;
     A. Di Domenico, et al., Found. Phys. 40 (2010) 852.
[38] V.A. Kostelecký, N. Russell, J. Tasson, Phys. Rev. Lett. 100 (2008) 111102;
     R. Lehnert, W.M. Snow, H. Yan, Phys. Lett. B 730 (2014) 353.
[39] V. Barger, D. Marfatia, K. Whisnant, Phys. Lett. B 653 (2007) 267;
     P. Adamson, et al., Phys. Rev. Lett. 105 (2010) 151601;
     A.G. Cohen, S.L. Glashow, Phys. Rev. Lett. 107 (2011) 181803;
     V.A. Kostelecký, M. Mewes, Phys. Rev. D 85 (2012) 096005;
     T. Katori, Mod. Phys. Lett. A 27 (2012) 1230024;
     J.S. Díaz, V.A. Kostelecký, R. Lehnert, Phys. Rev. D 88 (2013) 071902.
[40] V.A. Kostelecký, R. Lehnert, Phys. Rev. D 63 (2001) 065008;
     C. Adam, F.R. Klinkhamer, Nucl. Phys. B 657 (2003) 214;
     C.M. Reyes, L.F. Urrutia, J.D. Vergara, Phys. Rev. D 78 (2008) 125011;
     M.A. Hohensee, D.F. Phillips, R.L. Walsworth, arXiv:1210.2683 [quant-ph];
     D. Colladay, P. McDonald, R. Potting, Phys. Rev. D 89 (8) (2014) 085014;
     C. Hernaski, Phys. Rev. D 90 (12) (2014) 124036.
[41] V.A. Kostelecký, C.D. Lane, A.G.M. Pickering, Phys. Rev. D 65 (2002) 056006;
     G. de Berredo-Peixoto, I.L. Shapiro, Phys. Lett. B 642 (2006) 153;
     D. Colladay, P. McDonald, Phys. Rev. D 79 (2009) 125019;
     D. Colladay, P. McDonald, Phys. Rev. D 77 (2008) 085006;
     D. Colladay, P. McDonald, Phys. Rev. D 75 (2007) 105002;
     A. Ferrero, B. Altschul, Phys. Rev. D 84 (2011) 065030.
[42] D. Colladay, P. McDonald, J. Math. Phys. 43 (2002) 3554;
     R. Lehnert, Phys. Rev. D 74 (2006) 125001;
     R. Lehnert, Rev. Mex. Fis. 56 (2010) 469;
     B. Altschul, J. Phys. A 39 (2006) 13757.
[43] R. Jackiw, V.A. Kostelecký, Phys. Rev. Lett. 82 (1999) 3572;

     M. Pérez-Victoria, Phys. Rev. Lett. 83 (1999) 2518;
     R. Lehnert, J. Math. Phys. 45 (2004) 3399;
     B. Altschul, Phys. Rev. D 73 (2006) 036005;
     Q.G. Bailey, V.A. Kostelecký, Phys. Rev. D 74 (2006) 045001;
     A.J. Hariton, R. Lehnert, Phys. Lett. A 367 (2007) 11;
     V.A. Kostelecký, J.D. Tasson, Phys. Rev. D 83 (2011) 016013;
     R. Potting, Phys. Rev. D 85 (2012) 045033;
     M. Cambiaso, R. Lehnert, R. Potting, Phys. Rev. D 85 (2012) 085023;
     M. Cambiaso, R. Lehnert, R. Potting, Phys. Rev. D 90 (6) (2014) 065003;
     M. Schreck, Phys. Rev. D 89 (10) (2014) 105019;
     M. Schreck, Phys. Rev. D 90 (8) (2014) 085025.
[44] V.A. Kostelecký, N. Russell, Phys. Lett. B 693 (2010) 443.
[45] G. Randers, Phys. Rev. 59 (1941) 195.
[46] T. Sunada, in: Proc. KAIST Math. Workshop, vol. 8, 1993, p. 93;
     Z. Shen, Can. J. Math. 55 (2003) 112;
     D. Bao, C. Robles, Z. Shen, J. Differ. Geom. 66 (2004) 377;
     D. Bao, C. Robles, in: D. Bao, R.L. Bryant, S.-S. Chern, Z. Shen (Eds.), A Sampler
     of Riemann–Finsler Geometry, Cambridge University Press, Cambridge, 2004;
     G.W. Gibbons, C.A.R. Herdeiro, C.M. Warnick, M.C. Werner, Phys. Rev. D 79
     (2009) 044022.
[47] B. Winstein, in: K. Winter (Ed.), Festi-Val — Festschrift for Val Telegdi, Elsevier,
     Amsterdam, 1988;
     J.L. Rosner, Am. J. Phys. 64 (1996) 982;
     J.L. Rosner, S.A. Slezak, Am. J. Phys. 69 (2001) 44;
     V.A. Kostelecký, A. Roberts, Phys. Rev. D 63 (2001) 096002;
     M. Caruso, H. Fanchiotti, C.A. Garcia Canal, Ann. Phys. 326 (2011) 2717;
     K.R. Schubert, J. Stiewe, J. Phys. G 39 (2012) 033101;
     A. Reiser, K.R. Schubert, J. Stiewe, J. Phys. G 39 (2012) 083002.
[48] See, e.g., C. Barceló, S. Liberati, M. Visser, Living Rev. Relativ. 8 (2005) 12;
     C. Barceló, S. Liberati, M. Visser, Living Rev. Relativ. 14 (2011) 3.
[49] See, e.g., J. Schindler, et al., Phys. Rev. A 84 (2011) 040101(R);
     C.M. Bender, B.K. Berntson, D. Parker, E. Samuel, Am. J. Phys. 81 (2013) 173.
[50] M. Matsumoto, Tensor, NS 24 (1972) 29;
     M. Matsumoto, S. Hōjō, Tensor, NS 32 (1978) 225.
[51] D. Colladay, private communication.
[52] See, e.g., J.D. Jackson, Classical Electrodynamics, 3rd edition, John Wiley & Sons,
     New York, 1998.